

See discussions, stats, and author profiles for this publication at: <https://www.researchgate.net/publication/231645245>

Atomic Force Microscopy Studies of Carbon Nitride (CN_x) Films Deposited on a Conducting Polymer Substrate

ARTICLE *in* THE JOURNAL OF PHYSICAL CHEMISTRY C · OCTOBER 2010

Impact Factor: 4.77 · DOI: 10.1021/jp103795c

CITATIONS

10

READS

39

5 AUTHORS, INCLUDING:



Claude Deslouis

Pierre and Marie Curie University - Paris 6

174 PUBLICATIONS 3,247 CITATIONS

SEE PROFILE

Atomic Force Microscopy Studies of Carbon Nitride (CN_x) Films Deposited on a Conducting Polymer Substrate

J. C. Byers,[†] P. Tamiasso-Martinhon,^{‡,§,||} C. Deslouis,^{‡,§} A. Pailleret,^{*,‡,§} and O. A. Semenikhin^{*,†}

Department of Chemistry, The University of Western Ontario, London, Ontario, N6A 5B7, Canada, CNRS, UPR 15, Laboratoire Interfaces et Systèmes Electrochimiques, (LISE, case courrier 133), 4 Place Jussieu, F-75005, Paris, France, UPMC Univ. Paris VI, UPR 15, Laboratoire Interfaces et Systèmes Electrochimiques, (LISE, case courrier 133), 4 Place Jussieu, F-75005, Paris, France, and Centro de Desenvolvimento Tecnológico em Saúde CDTS-FIOCRUZ, Av. Brasil, 4365, Manginhos, CEP: 21040-900, Rio de Janeiro, RJ, Brasil

Received: April 27, 2010; Revised Manuscript Received: September 16, 2010

Carbon nitride films were deposited onto indium tin oxide and undoped polybithiophene substrates using direct-current reactive magnetron sputtering. The local morphology and electronic properties of the deposited films were investigated using phase-imaging (PI-AFM) and current-sensing atomic force microscopy (CS-AFM). The deposited materials were found to be generally amorphous with many individual nanostructured bonding domains. The nature of the substrate was found to have a significant effect on the microscopic distribution of carbon nitride regions with the carbon nitride films showing some long-range order when deposited onto an undoped polybithiophene substrate.

1. Introduction

Carbon films are a fascinating class of materials that display a wide range of interesting physical properties, making them promising candidates for numerous applications. The variation in their physical properties results from the different bonding arrangements of carbon in the films. Furthermore, these materials can be modified by the incorporation of various elements to alter their electronic and/or mechanical properties, as in the case of boron-doped diamond (BDD) and amorphous carbon nitride (a-CN_x), thus broadening the scope of applications from sensors and electrode materials to organic semiconductors and electron emitters.^{1,2} Whereas boron-doped diamond is a relatively well studied material as both a conducting coating or electrode material for degradation of organic pollutants, carbon nitride (CN_x) materials are considerably less investigated.^{3,4} It was shown that nitrogen can act as effective n-type modifier in carbon materials^{5–7} making CN_x potential n-type semiconductor materials.

Tetrahedral amorphous carbon (ta-C) is made up of a predominantly diamond-like sp³ network containing small graphite-like sp² clusters. The sp² bonded carbon clusters strongly influence the electronic properties of this material. Whereas diamond is an insulator with a band gap of 5.5 eV, tetrahedral amorphous carbon is a p-type semiconductor with a band gap of 2–2.2 eV due to the presence of π states.⁵ The incorporation of nitrogen into ta-C can lead to variations of conductivity that result from changes in band gap or band tailing.⁸ This conductivity increase with nitrogen in a-C is much less because native a-C is mainly sp² based and shows a maximum value for a low nitrogen content correlated to a

maximum in the intensity of the G band of the Raman spectrum.⁹ As was shown in the literature, the introduction of nitrogen can result in many different possible bonding arrangements between nitrogen and carbon,^{6,10} including σ - and π -bonding.

A nitrogen atom contains five valence electrons and it can use three of these electrons to form three sp² bonds. The remaining two electrons form a nonbonding lone pair in a π orbital. In this case, the π^* orbital is empty and n-type conductivity does not occur. The result is the formation of pyridine-like and pyrrole-like bonding configurations in the graphitic network. For nitrogen to act as an n-type modifier, it must substitute a graphitic carbon atom leading to three electrons being used to form three σ bonds, one electron from carbon along with one electron from nitrogen filling the π state, and the remaining electron going into the π^* state leading to n-type conductivity.⁶ With an increase in the nitrogen content, more carbon atoms are transformed from the sp³ to the sp² configuration. This is accompanied by an increased disorder that allows for the relaxation of mechanical stresses in the film.^{11,12} The electrical properties of carbon nitride films are influenced by the relative abundance of these sp² regions as well as the local bonding between nitrogen and carbon in the sp² regions.¹³

In this work, we were interested in studying the effect of the substrate on the properties of vacuum-deposited carbon nitride films. Specifically, we selected indium tin oxide (ITO) and undoped polybithiophene (PBT) substrates to examine their influence on the resulting morphology and electronic properties of the carbon nitride films. Polybithiophene is a well-known π -conjugated organic material with a dominance of organic π (sp²) bonding. It was of interest to investigate how the presence of extended π -conjugation in the substrate affects the properties and structure of the deposited carbon nitride films. In addition, as PBT is a p-doped conducting polymer and a-CN_x is an n-type semiconductor with a 2 eV band gap, this gives an example of an original organic–inorganic n–p type junction. The studies of the local morphology and electrical properties were carried out using atomic force microscopy (AFM) and its extensions, current-sensing AFM (CS-AFM) and phase imaging (PI-AFM).

* To whom correspondence should be addressed. E-mail: osemenik@uwo.ca. Phone: +1 519 661 2111ext. 82858. Fax: +1 519 661 3022 (O.A.S.), E-mail: alain.pailleret@upmc.fr. Phone: + 33 01 44 27 41 69. Fax: + 33 01 44 27 40 74 (A.P.).

[†] Department of Chemistry, The University of Western Ontario.

[‡] CNRS, UPR 15, Laboratoire Interfaces et Systèmes Electrochimiques.

[§] UPMC Univ. Paris VI, UPR 15, Laboratoire Interfaces et Systèmes Electrochimiques.

^{||} Centro de Desenvolvimento Tecnológico em Saúde CDTS-FIOCRUZ.

The composition and bonding of the CN_x films were characterized by X-ray photoelectron spectroscopy (XPS).

2. Experimental Section

2.1. Reagents and Apparatus. Bithiophene (BT) was purchased from Sigma-Aldrich and purified through vacuum sublimation. Tetrabutylammonium hexafluorophosphate (Sigma-Aldrich, 98% purity, reagent grade) was used as received. Acetonitrile was purified using an SPS-400-5 (Innovative Technology) solvent purification system. A Princeton Applied Research (PAR 263A) potentiostat-galvanostat controlled by CorrWare electrochemical software (Scribner Associates Inc.) was used for electrochemical deposition.

2.2. Electrode Preparation. Indium tin oxide covered glass electrodes were purchased from Delta Technologies, Ltd. (Stillwater, MN, USA) and had a surface resistance of 15–25 Ω /square. The electrodes were cleaned by sonicating in successive solutions of a detergent, deionized water, acetone, ethanol, and deionized water. The electrodes were dried using nitrogen gas to avoid water spotting and placed in an oven at 80 °C for 4 h.

PBT films were deposited onto indium tin oxide electrodes through electropolymerization. This was performed in a three electrode Pyrex glass cell without separation of the anodic and cathodic compartments. Galvanostatic deposition at a current density of 1 mA cm⁻² was used. The cells were purged with Ar gas prior to deposition. During deposition the gas was shut off and the cells were completely sealed. The electrochemical polymerization cell contained 5 \times 10⁻³ M of the BT monomer and 0.1 M Bu₄NPF₆ as the supporting electrolyte. The electrodeposited PBT layers thus produced in the reduced state covered approximately half of the ITO glass electrode. After the deposition, electrodes were rinsed three times in pure acetonitrile to remove residual monomer and electrolyte and dried under vacuum to remove the residual solvent.

2.3. Carbon Nitride Deposition. The carbon nitride (CN_x) films on ITO and reduced PBT were prepared by dc sputtering in an Ar/N₂ atmosphere with a total chamber pressure of 1 Pa. Let us note that the use of dc sputtering technique for deposition of CN_x films is more suitable to industrial applications as inexpensive and processable on large areas. The nitrogen partial pressure was kept constant at 15% of the total pressure using a mass flow controller. This has been previously reported to result in an atomic nitrogen content of approximately 0.20 ($x = 0.20$ in CN_x).⁹ Films were sputtered for 20 min at a power of 50 W onto indium tin oxide substrates partially coated with reduced PBT, as described above. A 50 W power was chosen because it allows avoiding etching or damages of the substrate due to high-energy bombardment during the deposition phase. The deposition was performed through a keyhole-shaped mask so that, in each growth experiment, a portion of the CN_x film was deposited on the ITO substrate coated with reduced PBT, whereas the other portion of the same CN_x film was deposited onto bare ITO. This procedure allowed us to perform an accurate comparison of the properties of the CN_x films and the effects of the substrate. It may be emphasized that the different involved materials have quite different conductivities from around 10³ S/cm for ITO (compatible with the surface resistance given above) to 10⁻² ~ 1 S/cm for a-CN_x and presumably less for undoped PBT, a fact that might have an impact on the growth mechanisms due to the dc sputtering technique. With this set of sputtering parameters, the thickness of the a-CN_x films is expected to be approximately 70 nm (estimation extracted from unpublished results) on condition that the substrate be a doped

silicon substrate (resistivity, 10⁻³ to 5 \times 10⁻³ Ω .cm). It is likely that the conductivity of the substrate (ITO or undoped PBT) somehow influences the deposition rate, especially in our case where the sputtering deposition is carried out in dc conditions.

2.4. Atomic Force Microscopy. Tapping mode, phase imaging AFM (PI-AFM) and current sensing AFM (CS-AFM) measurements were performed in ambient conditions using a Multimode AFM (Veeco Metrology) equipped with a Nanoscope IV controller (Veeco) and a CS-AFM extension module. Silicon PointProbe tips (NanoWorld, typical resonant frequency 320 kHz, typical force constant 42 N/m) were used for tapping mode and phase imaging. DDESP conducting diamond coated AFM probes (Nanoworld, typical force constant 0.35 N/m) were used for CS-AFM experiments.

Phase imaging AFM (PI-AFM) is an extension of regular tapping mode AFM. In phase imaging, variations in the phase of the cantilever vibrations are recorded simultaneously with topography imaging and are used to study the mechanical properties of the films. The phase of a cantilever in contact with the sample surface will be shifted with respect to the phase of a freely vibrating cantilever. The differences in phase can be used to map out regions of different crystallinity or density. Elastic interactions between the tip and sample, which are indicative of more crystalline or harder regions of the sample, lead to less negative or zero phase shifts, and will appear as brighter regions in the phase image.^{14,15} On the other hand, inelastic interactions between the tip and the sample lead to some energy dissipation and produce a relatively more negative phase shift. This happens over amorphous or softer regions of the sample, which then appear as darker regions in the phase image.

Current sensing AFM is a contact mode technique that measures the local superficial conductivity between the sample and a conducting AFM tip. These measurements can be performed while topography data are collected generating concurrent images of the local morphology and conductivity of the sample. A bias is applied to the tip and the flow of current between the tip and sample is measured at each point along the surface of the sample. In all CS-AFM experiments reported in this work, a bias of 500 mV was applied to the tip with respect to the sample and therefore the conducting regions (regions of higher positive currents) appear bright in these images (the positive current direction is from the sample into the tip).

3. Results and Discussion

Figure 1 shows representative scanning electron microscope (SEM) images of a PBT substrate with and without a carbon nitride film deposited onto the surface. The morphology of the PBT substrate shown in part a of Figure 1 is consistent with numerous microscopic data for this polymer and displays polymer grains with the sizes on the order of 30–50 nm.^{15–17} Deposition of a CN_x film does not substantially modify the general morphology of the substrate (part b of Figure 1): it appears that each polymer globule is coated with the CN_x film. Similar results were obtained by SEM studies of CN_x films deposited on ITO: although the ITO substrate morphology was very different from that of PBT, the deposited carbon films followed the morphology of the substrate. To investigate this further, PI-AFM and CS-AFM were used to examine respectively the nanoscale morphology and conductivity of the ITO and reduced PBT substrates as well as CN_x films deposited on these substrates. The ITO substrate was used as a reference because the CN_x films obtained on this substrate were very similar to those described in the literature and thus can be

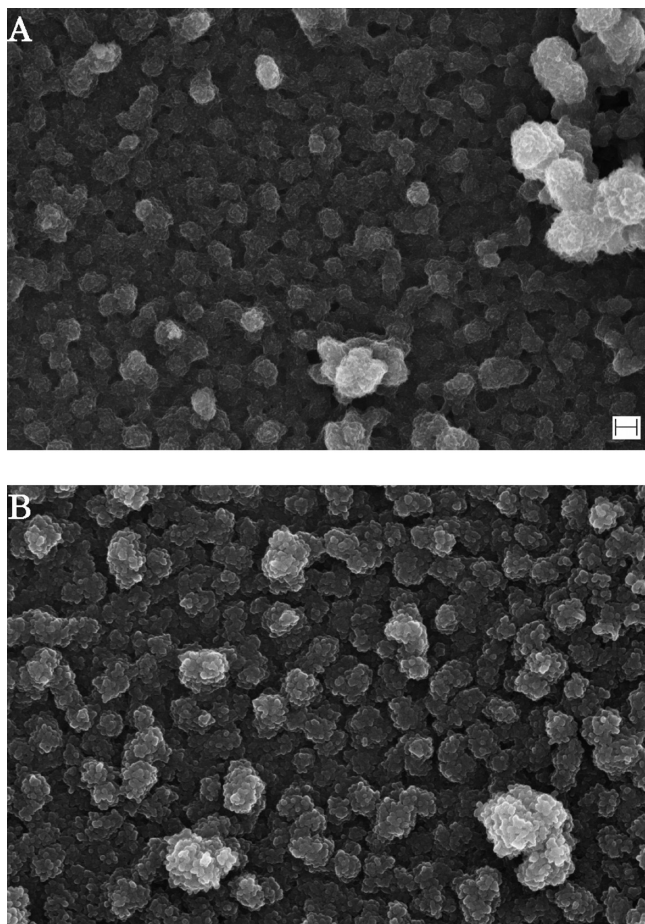


Figure 1. SEM-FEG images of (A) undoped polybithiophene substrate and (B) carbon nitride deposited on an undoped polybithiophene substrate. Scale bar shown in part A is applicable to both parts A and B and corresponds to 200 nm.

considered typical for films obtained on inorganic, non- π -conjugated, substrates.¹⁸ Furthermore, as has been already noted, the CNx coating was deposited simultaneously onto both the ITO and the reduced PBT substrates in the same experiment, allowing us to confidently relate the differences in the CNx film properties to the substrate and not the CNx deposition parameters.

3.1. Carbon Nitride Films on ITO. Figure 2 displays representative images of topography, phase (part b of Figure 2), and CS-AFM current (part d of Figure 2) obtained for a CNx film deposited onto an ITO substrate. For the sake of comparison, images of the same ITO substrate without the CNx film are also shown in parts a and c of Figure 2. Each measurement is presented as a pair of images, one of which (left) represents the topography, and the other (right) shows either the phase or the CS-AFM current, measured simultaneously with the sample topography. The bare ITO film features island-like structures comprised of very small individual grains, as can be seen in the topography images of parts a and c of Figure 2. From the phase image of part a of Figure 2 it can be seen that the ITO substrate grains consist of hard grain cores surrounded by softer periphery. There is a good correlation between the topography and the phase images. The CS-AFM measurements (part c of Figure 2) show that the grain cores are very conductive, whereas the rest of the material is considerably less conductive. These patterns probably reflect the variations in the chemical composition or the doping level of the indium tin oxide films.¹⁹

The image on the left-hand side of part b of Figure 2 shows the topography of a carbon nitride film deposited onto the ITO

substrate. The topography images of parts a and b of Figure 2 are fundamentally quite similar, with the CNx film following the topography of the ITO substrate. However, the phase image (the right-hand side of part b of Figure 2) clearly shows the CNx film to be less heterogeneous as there is much less variation in the phase values between the cores and the periphery of individual grains. These data indicate that CNx is deposited on top of each of the ITO grains and forms a relatively uniform film. This implies a 3D growth rather than columnar growth as both the conducting and less conducting zones of ITO are covered with a CNx film.

The CS-AFM image of the same CNx film deposited onto the ITO substrate is shown in part d of Figure 2. It can be seen in this image that the CNx film features a very pronounced variation of the electrical conductivity. Furthermore, there is a very clear correlation between the topography and the conductivity patterns: each conducting region in the CS-AFM image corresponds to a single grain of the material. At the same time, the conductivities of individual grains vary. The overall conductivity of the CNx film is much lower as compared to the ITO substrate (cf. the z-scale values for the CS-AFM current images of (c) and (d)), as was to be expected because the CNx films should be semiconducting at these values of the nitrogen content.²⁰ The formation of small conducting CNx grains correlates well with the patterns observed in the phase images of these films (part b of Figure 2). Taken together, the phase and the CS-AFM data show that deposition of CNx on ITO follows the morphology of the ITO substrate and occurs through the formation and growth of small hard conducting CNx nuclei on top of conducting ITO grains. As a result, each ITO grain becomes more or less uniformly coated with the CNx film. Whereas the phase and conductivity images show some variations among individual CNx grains, each grain features quite uniform phase and conductivity distributions.

3.2. Carbon Nitride Films on PBT. Figure 3 presents topography, phase and CS-AFM (current) images obtained for a CNx film deposited onto a conducting polymer (reduced PBT, parts b and d respectively of Figure 3) substrate. Again, as with the case of ITO, images of noncoated PBT are also shown in parts a and c of Figure 3. The noncoated PBT images were obtained within the sample area protected by the mask during the CNx deposition. For each measurement, a pair of images that represent the topography (left) and either the phase or the CS-AFM current (right) are shown. Part a of Figure 3 presents topography and phase images of the PBT substrate. It can be seen that the polymer grains are much larger than those of ITO. Furthermore, the polymer exhibits well-known cauliflower conglomerate formations typical for conducting polymer substrates.^{16,17,21} The size of such conglomerates is ca. 100–300 nm, whereas the size of individual polymer grains is ca. 30–50 nm.

The phase image of part a of Figure 3 shows that the cauliflower-like conglomerates of the PBT substrate have a complex structure. Specifically, they incorporate a number of smaller polymer grains with dense/crystalline cores and amorphous periphery, as was observed for this polymer previously.^{15,22} Additionally, harder circular regions along the boundaries of the polymer agglomerates are also visible in some areas. Part c of Figure 3 is a CS-AFM image of the PBT substrate. The conductivity of the substrate is quite low and features slight variations that correlate with the polymer morphology, as expected from the reduced state of PBT. This is consistent with previous investigations of the local electronic properties of native PBT substrates.²³

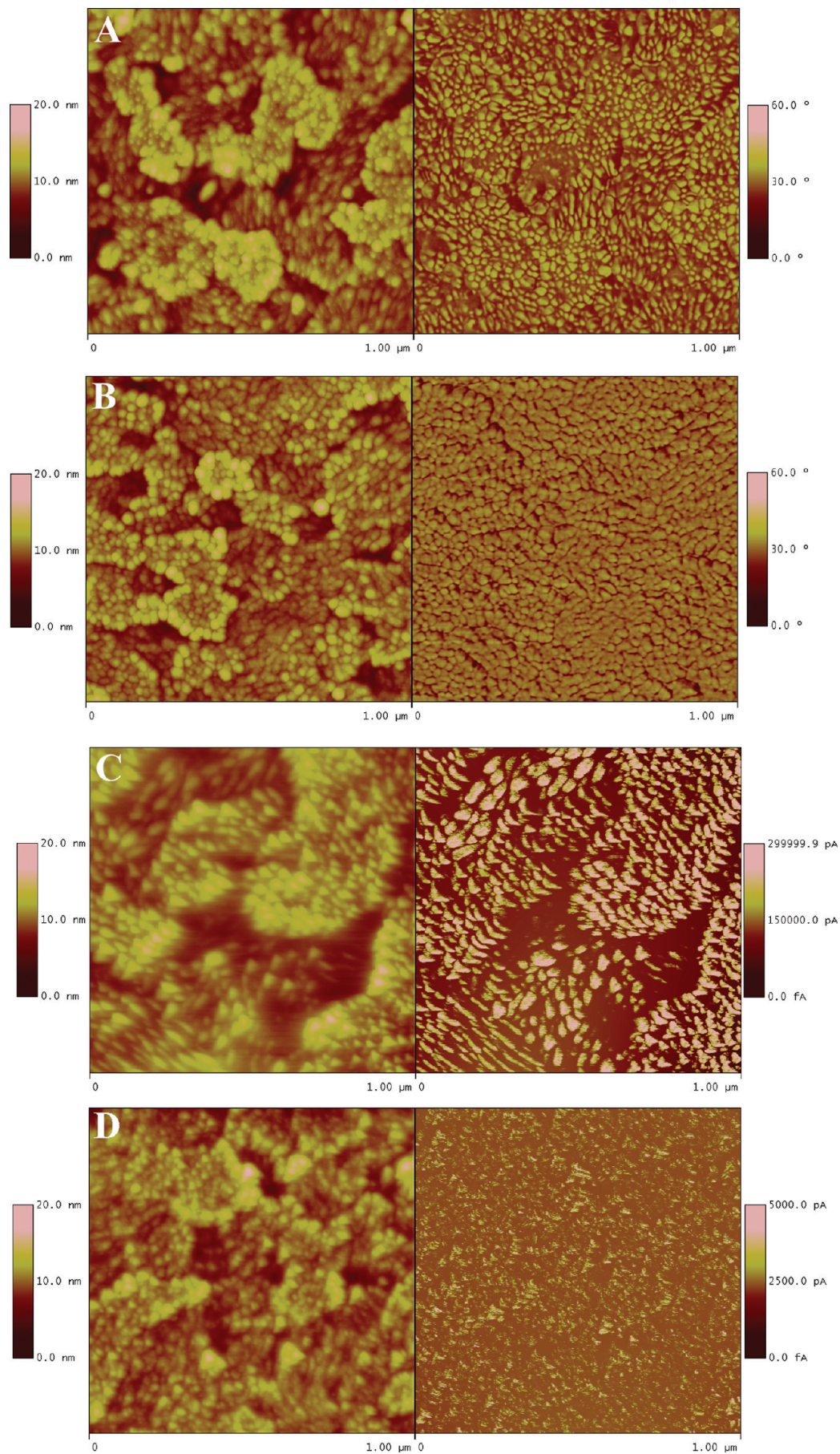


Figure 2. (A,B) 1 μm by 1 μm topography (left) and phase (right) AFM images of (A) ITO and (B) CN_x on ITO. (C,D) 1 μm by 1 μm topography (left) and CS-AFM current (right) images of (C) ITO and (D) CN_x on ITO. The Z-scales are: topography, 20 nm; phase, 60 $^\circ$; CS-AFM current, 300 nA for (C) and 5000 pA for (D). The applied tip bias was +500 mV.

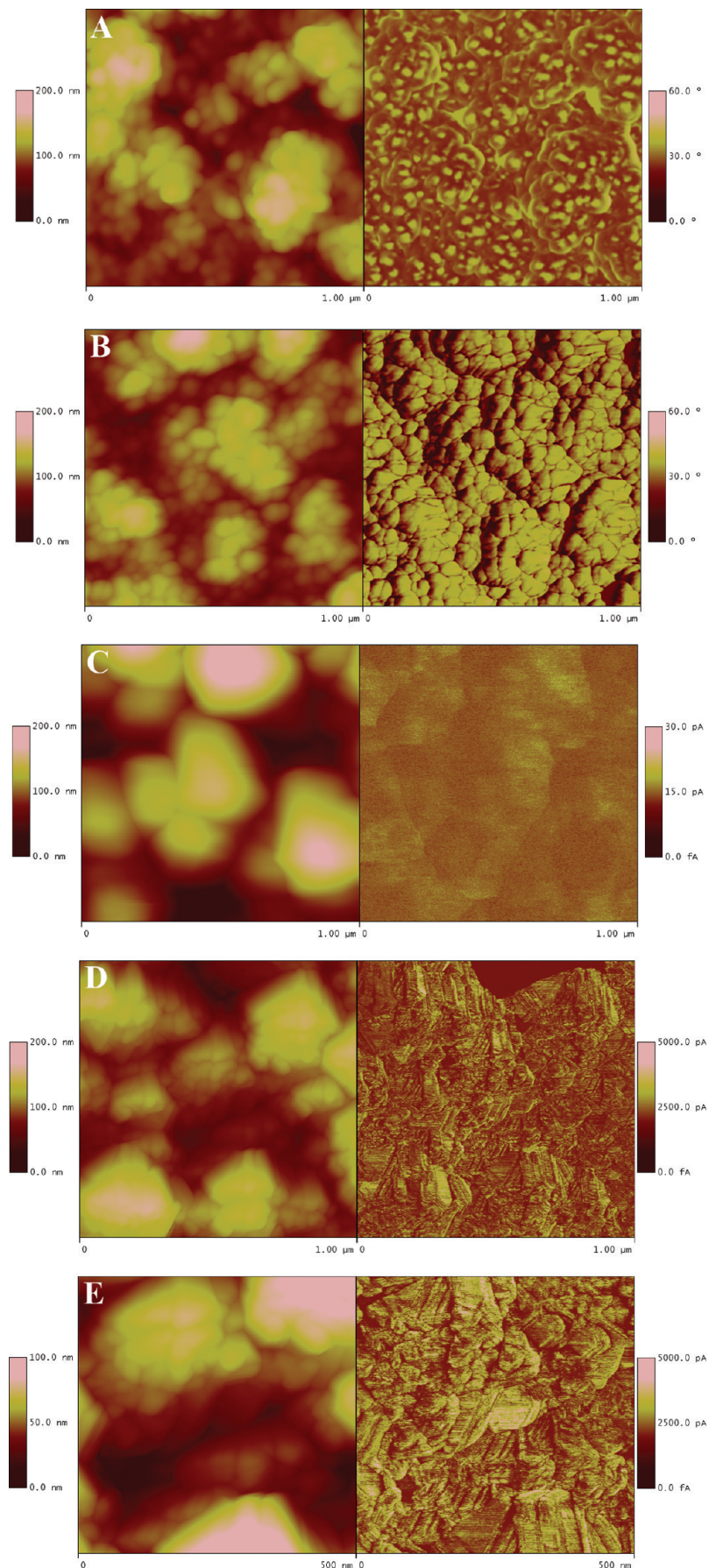


Figure 3. (A,B) 1 μm by 1 μm topography (left) and phase (right) AFM images of (A) PBT and (B) CNx on PBT. (C,D) 1 μm by 1 μm topography (left) and CS-AFM current (right) images of (C) PBT and (D) CNx on PBT. (E) Enlarged 500 nm by 500 nm image of topography (left) and CS-AFM current (right) of CNx on PBT. The Z-scales are: topography, 200 nm; phase, 60°; CS-AFM current, 30 pA for (C) and 5000 pA for (D,E). The applied tip bias was +500 mV.

Part b of Figure 3 shows topography and phase images of a CN_x film deposited onto a PBT substrate. As with ITO, the deposited CN_x film follows the general topography of the PBT film. The phase image is absolutely different from that of the PBT substrate and is much more uniform, exhibiting a pattern similar to that observed for CN_x on ITO (part b of Figure 2), with the exception of much larger grain sizes in the case of CN_x on PBT. This suggests that, similarly to CN_x on ITO, CN_x on PBT forms a continuous and relatively homogeneous film across the PBT substrate. However, the local conductivity measurements for CN_x films on PBT (part d of Figure 3) show a distinct pattern, which is markedly different from that observed for CN_x films deposited onto ITO substrates. Instead of round conducting domains that more or less follow the morphology of the substrate, the conductivity distribution for CN_x on PBT displays linear or layered conductivity patterns that do not have any notable correlation to the film morphology. At the same time, they show definite signs of long-range ordering. This is especially evident from the high-resolution image of part e of Figure 3. Furthermore, in many instances such linear conductivity patterns extend beyond the corresponding grains of the material. Because these effects were not observed for the ITO substrate, the observed behavior is attributed to the conjugated polymer substrate.

Generally speaking, the variations in the local conductivity of the CN_x films can occur due to microscopic variations in the bonding arrangements of nitrogen and carbon atoms. The less conducting regions may represent sp³ bonded carbon and nitrogen.²⁴ The electronic properties of a CN_x film containing a large amount of nitrogen are determined by the π and π^* states. These states arise from sp² C=C bonds in graphite and sp² C=N bonds in pyrrole-like, pyridine-like, and nitrogen-substituted graphite fragments. It has been previously suggested that the introduction of nitrogen into an amorphous carbon film leads to formation and clustering of sp² fragments up to a certain level of nitrogen.^{6,12} Specifically, with increasing nitrogen content, formation of sp² C=N and sp³ C-N bonds at the expense of sp² C=C bonds is favored.²⁴ The highly conducting regions (the brightest areas in parts d and e of Figure 3) observed on CN_x deposited on undoped PBT are probably graphitic regions in the film that do not contain nitrogen.²⁵ The moderately conducting regions (less bright areas) are attributed to sp² regions containing carbon nitride. They display semiconducting properties and are likely to be more disordered due to the incorporation of nitrogen into the graphitic region.²⁰ The insulating regions (dark areas) can be attributed to regions with nonconjugated sp³ C-N bonding,²⁴ or to regions with high nitrogen content.

Therefore, the conductivity distribution observed in parts d and e of Figure 3 can be related to the distribution of various bonding patterns in CN_x films. First of all, the sp² content could be influenced by a reaction with the π -conjugated PBT substrate. Because this organic substrate is soft and could become reactive under the conditions found in the deposition chamber (plasma, elevated temperature, bombardment with nitrogen/carbon/argon ions), it could be suggested that the substrate would react with the depositing carbon films forming some kind of strong interactions not found in CN_x films deposited on inorganic substrates such as ITO. Specifically, it would involve, in addition to the graphite, pyridine, and pyrrole moieties typical to CN_x films, also certain thiophene or related fragments, thus affecting the sp² content. However, in this case, the CN_x films would have contained a noticeable amount of sulfur from the thiophene moieties. To check for this, CN_x films were subjected to XPS analysis, and no traces of sulfur were found in CN_x films

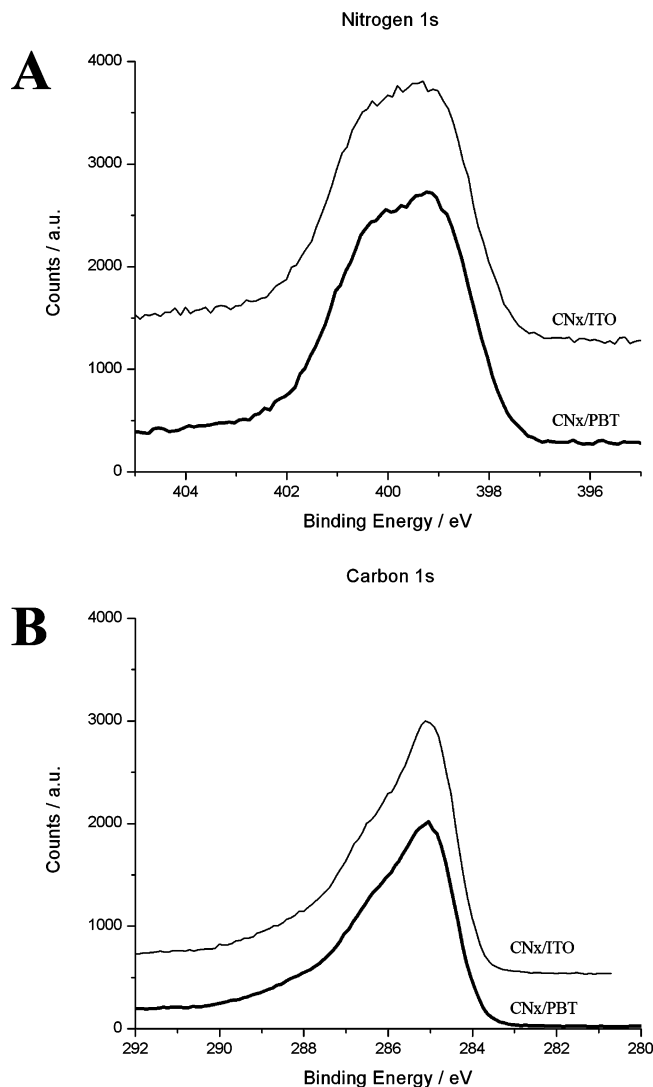


Figure 4. (A) Nitrogen 1s and (B) carbon 1s XPS spectra of CN_x on ITO and PBT.

deposited on PBT substrates. Furthermore, both the carbon and nitrogen regions of the XPS spectra were found to be very similar for films deposited on either of the substrates (Figure 4) indicating that the overall character of the adhesion process and the content of various carbon and nitrogen-containing moieties in the films did not depend on the deposition substrate, at least, within the limits of the XPS probe depth. Studies of the early stages of CN_x film deposition are required to further clarify this issue. Furthermore, the total absence of the sulfur signal in the XPS spectra demonstrates the CN_x films deposited on PBT are indeed continuous and cover 100% of the PBT substrate.

Therefore, whereas the overall chemical composition and adhesion process of CN_x films deposited on ITO and PBT are very similar as revealed by XPS, pronounced differences in the local conductivity patterns demonstrated by the CS-AFM measurements suggest that the substrate affects the microscopic distribution of the various types of chemical compositions in CN_x films. This can arise from differences in the kinetics and mechanism of nucleation and growth of CN_x films on ITO and PBT. For the ITO substrate, nucleation of a carbon film occurs on a structurally and energetically foreign surface. In this case, nucleation is a rate-determining step, which would lead to formation of a few very small nuclei. The distribution of the

primary nuclei is likely to be markedly affected by the current and thus ion flux distribution in the deposition chamber and therefore by the local variations in the conductivity of the substrate. As a result, nucleation is most probable on the highly conducting cores of ITO grains, which explains the correlation of topography and conductivity of the deposited CNx films with the morphology and conductivity of the ITO substrate. At a later stage, the nuclei grow forming a relatively uniform film.^{26,27}

For PBT substrate, a weak variation in the conductivity is observed that does not directly correspond to the morphology. Furthermore, nucleation in this case occurs on an organic and thus relatively less foreign substrate and therefore could be much easier (the nucleation is not the rate-determining step), with the deposited material complementing the existing features of the substrate. Additionally, the deposited material may apply its surface stress to the soft organic film.²⁸ As a result, growth of CNx on PBT could occur more easily, facilitating the formation of extended linear or layered patterns. To a certain extent, this process can be compared to the well-known heteroepitaxial growth, whereby the structure of the substrate influences the structure of the deposited material.²⁹ In this case, it is possible that the observed extended linear/layered patterns indicate the formation of at least partially crystalline materials. Normally, carbon nitride films are amorphous;³⁰ however, formation of such patterns as shown by our AFM data does indicate a certain degree of long-range order in the CNx films on PBT. Future studies using X-ray or electron diffraction are needed to further investigate this hypothesis. However, our results clearly demonstrate that the substrate has a very pronounced influence on the properties of vacuum-deposited CNx films.

4. Conclusions

The nanoscale morphology and conductivity of carbon nitride (CNx) films was found to be highly dependent on the substrate. CNx films deposited onto an inorganic substrate (ITO coated glass) showed the formation of conductivity patterns closely resembling those of the substrate. This can be related to the influence of the substrate conductivity on the current distribution in the deposition chamber. However, CNx films deposited onto a π -conjugated organic polymer (reduced PBT) substrate demonstrated very particular linear or layered local conductivity patterns, which did not follow either the morphology or the conductivity patterns for the substrate and indicated a possible formation of a semicrystalline structure. Such behavior was attributed to a difference in the kinetics of nucleation and growth of CNx films on ITO and PBT substrates and possibly to surface stress relaxation that is possible on a soft material (like undoped PBT) only. Investigations of the effects of the sputtering parameters (current, voltage, and duration) are also needed to define the influence of these parameters on the properties of CNx films as well as their homogeneity.

Acknowledgment. The support of this work by the Natural Sciences and Engineering Research Council of Canada (NSERC), Canada Foundation for Innovation/Ontario Innovation Trust (CFI/OIT), the Academic Development Fund of the University

of Western Ontario, and the University of Pierre and Marie Curie (UPMC, Paris, France) is gratefully acknowledged. The authors are grateful to Surface Science Western and personally to Mr. M. Biesinger for help with XPS measurements. Mr S. Borenstajn is warmly acknowledged for his expertise in SEM-FEG observations. One of the authors (O.A.S.) is grateful to UPMC for support of his visit to UPMC as an invited professor.

References and Notes

- (1) Swain, G. M.; Ramesham, R. *Anal. Chem.* **1993**, *65*, 345–351.
- (2) Yoo, K. S.; Miller, B.; Kalish, R.; Shi, X. *Electrochem. Solid-State Lett.* **1999**, *2*, 233–235.
- (3) Panizza, M.; Cerisola, G. *Electrochim. Acta* **2005**, *51*, 191–199.
- (4) Tamiasso-Martinhon, P.; Cachet, H.; Debieuvre-Chouvy, C.; Deslouis, C. *Electrochim. Acta* **2008**, *53*, 5752–5759.
- (5) Veerasamy, V. S.; Yuan, J.; Amaratunga, G. A. J.; Milne, W. I.; Gilkes, K. W. R.; Weiler, M.; Brown, L. M. *Phys. Rev. B* **1993**, *48*, 17954–17959.
- (6) Robertson, J.; Davis, C. A. *Diamond Relat. Mater.* **1995**, *4*, 441–444.
- (7) Davis, C. A.; McKenzie, D. R.; Yin, Y.; Kravtchinskaya, E.; Amaratunga, G. A. J.; Veerasamy, V. S. *Philos. Mag. B* **1994**, *69*, 1133–1140.
- (8) Ikeda, T.; Teii, K.; Casiraghi, C.; Robertson, J.; Ferrari, A. C. *J. Appl. Phys.* **2008**, *104*, 6002–6008.
- (9) Lagrini, A.; Charvet, S.; Benlahsen, M.; Debieuvre-Chouvy, C.; Deslouis, C.; Cachet, H. *Thin Solid Films* **2005**, *482*, 41–44.
- (10) Rodil, S. E.; Muhl, S. *Diamond Relat. Mater.* **2004**, *13*, 1521–1531.
- (11) Hu, J. T.; Yang, P. D.; Lieber, C. M. *Phys. Rev. B* **1998**, *57*, R3185–R3188.
- (12) Ferrari, A. C.; Rodil, S. E.; Robertson, J. *Phys. Rev. B* **2003**, *67*, 155306.1–155306.20.
- (13) Monclus, M. A.; Cameron, D. C.; Chowdhury, A. K. M. S. *Thin Solid Films* **1999**, *341*, 94–100.
- (14) Magonov, S. N.; Reneker, D. H. *Annu. Rev. Mater. Sci.* **1997**, *27*, 175–222.
- (15) O'Neil, K. D.; Semenikhin, O. A. *J. Phys. Chem. C* **2007**, *111*, 14823–14832.
- (16) Barisci, J. N.; Stella, R.; Spinks, G. M.; Wallace, G. G. *Electrochim. Acta* **2000**, *46*, 519–531.
- (17) Chao, F.; Costa, M.; Jin, G.; Tian, C. *Electrochim. Acta* **1994**, *39*, 197–209.
- (18) Liu, D. P.; Benstetter, G. *Appl. Surf. Sci.* **2005**, *249*, 315–321.
- (19) Liao, Y. H.; Scherer, N. F.; Rhodes, K. J. *Phys. Chem. B* **2001**, *105*, 3282–3288.
- (20) Alibart, F.; Drouhin, O. D.; Benlahsen, M.; Muhl, S.; Rodil, S. E.; Camps, E.; Escobar-Alarcon, L. *Appl. Surf. Sci.* **2008**, *254*, 5564–5568.
- (21) Hien, N. T. L.; Garcia, B.; Pailleret, A.; Deslouis, C. *Electrochim. Acta* **2005**, *50*, 1747–1755.
- (22) Byers, J. C.; DiCarmine, P. M.; Moustafa, M. M. A.; Wang, X.; Pagenkopf, B. L.; Semenikhin, O. A. *J. Phys. Chem. B* **2009**, *113*, 15715–15723.
- (23) O'Neil, K. D.; Shaw, B.; Semenikhin, O. A. *J. Phys. Chem. B* **2007**, *111*, 9253–9269.
- (24) Benlahsen, M.; Cachet, H.; Charvet, S.; Debieuvre-Chouvy, C.; Deslouis, C.; Lagrini, A.; Vivier, V. *Electrochem. Commun.* **2005**, *7*, 496–499.
- (25) McCreery, R. L. *Chem. Rev.* **2008**, *108*, 2646–2687.
- (26) Logothetidis, S.; Gioti, M.; Patsalas, P. *Diamond Relat. Mater.* **2001**, *10*, 117–124.
- (27) Logothetidis, S. *Thin Solid Films* **2005**, *482*, 9–18.
- (28) Durand-Drouhin, O.; Benlahsen, M. *Solid State Commun.* **2004**, *131*, 425–429.
- (29) Campione, M.; Raimondo, L.; Moret, M.; Campiglio, P.; Fumagalli, E.; Sassella, A. *Chem. Mater.* **2009**, *21*, 4859–4867.
- (30) Hellgren, N.; Johansson, M. P.; Broitman, E.; Hultman, L.; Sundgren, J. E. *Phys. Rev. B* **1999**, *59*, 5162–5169.

JP103795C